

RADIOMETRIC PERFORMANCE OF AVIRIS: ASSESSMENT FOR AN ARID REGION GEOLOGIC TARGET

HUGH H. KIEFFER, ERIC M. ELIASON, KEVIN F. MULLINS, LAURENCE A. SODERBLOM, AND JAMES M. TORSON; U.S. Geological Survey, Flagstaff, Arizona, USA

ABSTRACT

Data from several AVIRIS flight lines were examined to assess instrument stability and response. Both scene and in-flight calibration data were analyzed statistically. The data clearly indicate that, although the instrument output was noisy and unstable at the time of data acquisition, valuable spectral signatures can still be extracted and analyzed. Some first order calibration corrections can be performed by forcing internal consistency within the data. AVIRIS data are delivered in band-interleaved-by-line format, but we have developed high-efficiency routines which access the data as either image or spectral planes and enable effective statistical and visual examination of both AVIRIS scenes and ancillary files.

Two methods were used to extract spectral information from segment 4 of the Kelso Dunes flight. Both successfully identified at least three distinct spectral signatures, but neither has positively identified a specific material.

INTRODUCTION

First, a detailed statistical analysis was performed on the various calibration files that accompany all AVIRIS flights for several 1987 targets (TABLE 1). Statistical parameters were collected for coherent and random noise patterns, offset and gain drifts, and intensity shifts; some or all of these problems exist in every flight line we investigated. These measures of performance were used to reject bands with low signal-to-noise ratios.

Table 1. Data Used in This Work

Flight Target	Date	Data Used
Moffett Field	6/25/87	Calib. only
Mountain Pass	7/30/87	Calib. only
Hebro	8/01/87	Calib. only
Sierra Foothills	9/14/87	Calib. only
Kelso Dunes	9/14/87	Calib. & image
Lake Powell	9/18/87	Calib. only
Grand Canyon	9/18/87	Calib. & image
San Francisco Bay	10/13/87	Calib. & image

NOISE LEVEL ANALYSIS

Pre- and post-flight calibration files were processed and average and standard deviation values were obtained for each of the four separate internal intensity levels (Figure 1). Histograms of raw DN and of the absolute second difference of the raw DN were generated. Using linear interpolation of the corresponding cumulative histograms, the 1 and 99 percentile points of the raw DN, and the median and mean absolute second difference were computed. Similar routines were run on the dark current and image files for Segment 4 of the Kelso Dunes flight. All analyses were done on raw AVIRIS data.

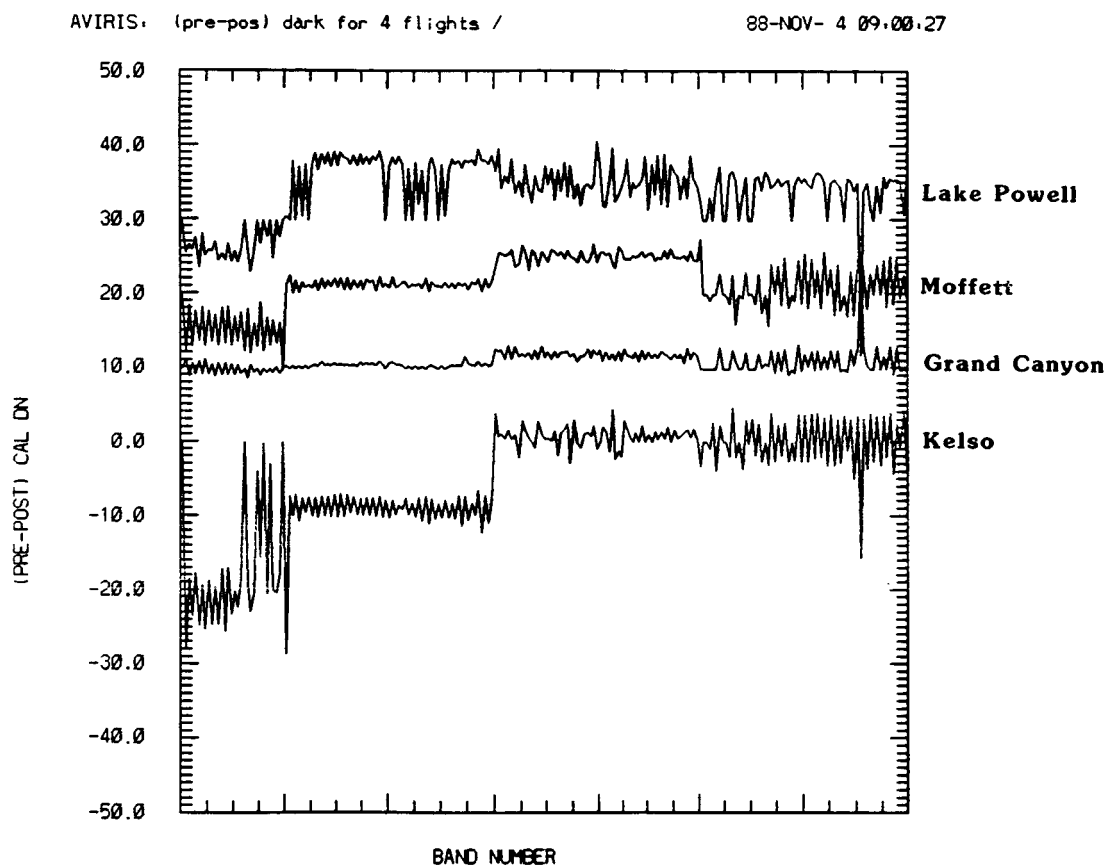


Figure 1. The difference between the pre- and post-calibration dark currents are compared for four AVIRIS flights. All four plots are actually centered on zero but each has been progressively offset vertically by 10 DN.

A simple measure of detector noise is one-half the median absolute value of the second difference (for Gaussian noise this is nearly identical to the standard deviation). This parameter varies strongly with detector, even within each of the four spectrometers. Typical values are 4.5, 2.5, 3.2, and 2.7 for spectrometers A, B, C and D, respectively. For the most responsive detectors in each spectrometer, the signal-to-noise ratio (SNR) for this measure of noise is approximately 150, 55, 100, and 60 for the four spectrometers. A revealing parameter is the "science-to-noise ratio", based on the variation of reflectivity within a scene,

ratioed to the noise level. This parameter is on the order of 20 to 30 for all four spectrometers.

There are several kinds of periodic noise within the AVIRIS data. In a wavelength "movie", waves with a period on the order of ten pixels flow across the image. In a uniform area (the ocean off the coast of Oregon) noise with the period of 14.16 pixels was shifted in phase by 10.5 samples between lines.

There are also several patterns of noise in the calibration data itself. The low-level pre-calibration data has an approximate square-wave pattern with amplitude of 4 to 6 DN with a period of 26 pixels. The dark level (1 pixel per line) shows high frequency noise, obvious, abrupt level shifts on the order of 5 pixels, and drifts on the order of a few DN per minute. In uniform scenes, some of the more obvious level shifts correspond to shifts in the dark current file.

COHERENT NOISE

Coherent noise was modeled by Fourier transforms of a uniform AVIRIS subscene and on-board calibration data acquired during the Kelso Dunes flight. A subscene of the dune field provided a uniform flat-field target for study of coherent noise at brightness levels above dark current. The on-board calibration consisted of instrument data acquired with the fore-optics shutter closed and the internal calibration lamp either turned off providing dark current data, or at high and low intensity levels providing a flat-field at different instrument DN output levels.

A one-dimensional fast Fourier transform (FFT) was applied to 512 samples of a line for all 224 spectral channels. Because a uniform-radiance field was used, amplitudes of all the Fourier components can be attributed to either random or coherent Fourier noise (except zero frequency). Typical background-frequency amplitudes due to random noise for the four spectrometers fall within the range .5 to 1.0 DN for most detectors. Some of the detectors with a lower signal-to-noise ratio have noticeably higher Fourier amplitudes at random frequencies. These include detectors 97, 113, 131 to 136, and 210.

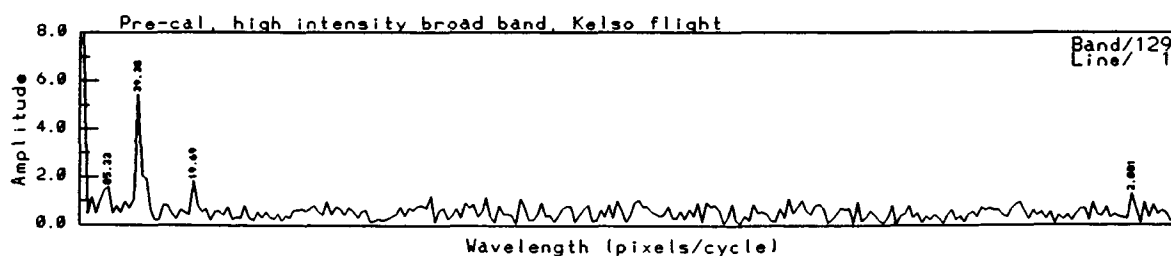


Figure 2. Fourier transform of the first 512 samples of a single scan line for detector C, band 129. The transform is of the Kelso Dunes flight pre-calibration data acquired with the fore-optics shutter closed and the internal calibration lamp at the high intensity level. Because a uniform-radiance field was used, the high-amplitude Fourier components can be attributed to coherent noise. The transform exhibits a sharp peak at 39.38 and 19.69 pixels/cycle and is typical of most of the detectors in spectrometer C.

The FFTs exhibited several sharp peaks well above background noise levels for the four spectrometers (see Table 2 and Figure 2). Because the coherent noise levels are approximately the same for the dark current calibration, low and high intensity lamp calibration, and image subscene, it is assumed to be an additive component to the signal and not a function of scene brightness.

In most cases all detectors of a spectrometer exhibited the same coherent noise frequency but with varying amplitude. Spectrometers A and B exhibited the lowest coherent noise levels of no larger than 2.0 DN amplitude. These noise patterns were not discernible above random noise levels when viewing a scene. Spectrometer D had slightly larger coherent noise levels of no larger than 4.0 DN amplitude. Visually, the 19.69 pixels/cycle coherent noise level was barely detectable above random noise levels in some detectors. Spectrometer C exhibited the greatest coherent noise levels and were visible well above the random noise levels. The 39.38 and 19.39 pixels/cycle coherent noise levels, having amplitudes as high as 8.0 and 4.0 DN respectively, were visible as oblique wave patterns.

TABLE 2. Summary of Fourier Transform Results

Spectrometer	Noise Frequency (pixels/cycle)	Maximum Amplitude (Raw DN)	Comments
A	19.69	1.8	Greatest in detectors 13, 16, 19, 22, 24, 25, 28, 30.
	2.12	2.0	Present in all detectors but minimal in 10, 30, 31, 32.
B	9.48	2.0	Amplitude nearly uniform in all detectors.
	5.70	1.8	Amplitude nearly uniform in all detectors.
C	39.38	8.0	Greatest in detectors 126 to 146. Amplitude varies widely among detectors.
	19.69	4.0	Greatest in detectors 131, 134, 139, 140, 145, 157.
D	32.00	3.0	Amplitude varies widely among detectors.
	19.69	4.0	Amplitude varies widely among detectors.

WHITE-TARGET MODEL

An estimate of the expected response of AVIRIS to a uniform point target was computed based on the calibration file supplied by JPL, a nominal atmospheric transmission spectrum computed using LOWTRAN 7 (Alee, 1988), and the solar spectrum. This resulted in a "WHITE" spectrum that was used to convert AVIRIS data to surface reflectance (Kieffer, 1988). Although attempts to derive normalized calibrated spectra using the model gave poor results, the model was useful in estimating the quality of different spectral regions based on expected atmospheric transmission and instrument performance.

An estimate of the relative gain of each band was computed by developing a "reference" band composed of the sum of DN for a spectrally contiguous set of low-noise, high-gain bands. A comparison of the coefficient of a linear least-squares fit of the data from any band to this reference band with that predicted by the white-target model gives a direct indication of the change of response of each detector.

SOFTWARE DISPLAY TOOLS

Given the large quantity of data produced by the AVIRIS instrument, a new system of software was designed to handle cube-formatted data. The software runs on a DEC Microvax Graphics Workstation interfaced to an IVAS display system. The display program, QL3, allows the user to interactively examine a three-dimensional cube of image data. The cube is displayed in two adjacent segments. The left-hand segment is an image of the surface (x,y) at a particular wavelength band which is defined by the location of the cursor in the spectral (z) dimension. The right-hand side is a spectral image representing all y pixels and all z bands within an orthogonal plane whose x location is defined by the cursor. A graph of the full spectrum at the x,y pixel is displayed on the workstation. Band images can be displayed singly with numerous color-coded overlay planes, or as a three color composite. Various options include panning, pseudo-coloration, normalization, stretching and listings of current display values.

The cube display software is designed to run with a number of concurrent processes that share access to the data in memory. These concurrent processes enable one to interactively collect and manipulate spectral data and store the results of several such analyses in tabular form for later processing. For example, pixels that match a selected spectrum can be identified and used to produce a thematic map or mask. A series of these thematic images, which may be color coded, can be overlaid on the original image to delineate (or mask out) areas with specific spectral characteristics.

DATA ANALYSIS

An attempt to extract subtle spectral variations along surfaces within the scene by suppressing instrument gain and offset errors and spectral variation in atmospheric transmission was made using the linear fit coefficients of each band to the "reference" band mentioned above. For each band, the response at each pixel was adjusted by the deviation of the reference band, at that pixel,

from the reference band average and scaled by the slope of the linear correlation between this band and the reference band. This process removed the instrument dark level and atmospheric additive terms, and variation in instrumental gain, solar spectral radiance and atmospheric transmission. It does not amplify noise, but it does remove any correlation of spectral signature with the local incidence angle. To whatever extent the reference bands do not represent the spectrally averaged brightness of surface materials, this process has the unfortunate characteristic of magnifying the spectral signature of the reference bands.

A second technique was developed to remove the instrument and atmospheric effects without use of any absolute calibration and was applied to a portion of the Kelso Dunes data set (Soderblom et al., in preparation). This process deals separately with the additive and multiplicative errors inherent in the AVIRIS data so that psuedo-spectral signals are not created by the normalization of the additive component.

The white-target spectrum mentioned earlier was used to mask out spectral regions of low response. Next, bands with excessive noise or data clipping were identified and deleted. The next step involved a process to detect and delete noisy spectra, with any spectrum being deleted that had a mean-squared deviation from both its left and right neighbors greater than 10 DN. If two spectra compared within this tolerance, then their average was stored. This cleaned-up data set was then used to generate histograms of all remaining channels and to compute the first and third quartiles. Finally, a linear stretch was applied to each spectral channel, that scaled the widths and centroids of all histograms to coincide. The signatures in the resulting spectra are dominated by the spectral character of the surface, not the spectral nature of the instrument or atmosphere. This process considerably improves the ability to discern individual ground units. We are now in the process of comparing the normalized spectral features identified in this manner with absolute laboratory spectra.

REFERENCES

- Alee, Ron, Feb. 2, 1988, Personal communication.
- Kieffer, H. H., April 19, 1988, Memorandum to AVIRIS project scientist.
- Soderblom, L. A. et al., in preparation, Data-Dependent Approaches For Correction and Analysis of AVIRIS Data